

SF2A 2006

D. Barret, F. Casoli, T. Contini, G. Lagache, A. Lecavelier, and L. Pagani (eds)

BENCHMARKING PDR MODELS AGAINST THE HORSEHEAD EDGE

Pety, J.¹, Goicoechea, J.R.², Gerin, M.², Hily-Blant, P.¹, Teyssier, D.³, Roueff, E.⁴, Habart, E.⁵ and Abergel, A.⁵

Abstract. To prepare for the unprecedented spatial and spectral resolution provided by ALMA and Herschel/HIFI, chemical models are being benchmarked against each other. It is obvious that chemical models also need well-constrained observations that can serve as references. Photo-dissociation regions (PDRs) are particularly well suited to serve as references because they make the link between diffuse and molecular clouds, thus enabling astronomers to probe a large variety of physical and chemical processes. At a distance of 400 pc (1" corresponding to 0.002 pc), the Horsehead PDR is very close to the prototypical kind of source (*i.e.* 1D, edge-on) needed to serve as a reference to models.

1 Introduction

Photodissociation region models are used to understand the evolution of the far UV illuminated interstellar matter both in our Galaxy and in external galaxies. To prepare for the unprecedented spatial and spectral capabilities of ALMA and Herschel, two different kinds of advances are currently taking place in the field. First, numerical models describing the chemistry of a molecular cloud are being benchmarked against each others to ensure that all models agree not only qualitatively but also quantitatively on at least simple cases (<http://www.ph1.uni-koeln.de/pdr-comparison>). Second, new or improved chemical rates are being calculated/measured by several theoretical and experimental groups. However, the difficulty of this last effort implies that only a few reactions (among the thousands used in chemical networks) can be thoroughly studied. This led to several recent studies trying to identify a few key chemical reactions in some well-studied astrophysical cases by comparison of “observed” and modelled abundances, taking into account both the observational and chemical rate uncertainties (*e.g.* Wakelam et al. 2004, 2006). In view of the intrinsic complexity of building reliable chemical networks and models, there is an obvious need of well-constrained observations that can serve as basic references. PDRs are particularly well suited to serve as references because they make the link between diffuse and dark clouds, thus enabling to probe a large variety of physical and chemical processes.

The Horsehead nebula, also known as Barnard 33, is one of the most famous object of the sky. For instance, it was selected by internet voters as a target for the Hubble Space Telescope in the framework of its 11th anniversary (See the Hubble Heritage site for details). But it is also a fantastic physical and chemical laboratory which has been actively studied in the past 5 years.

2 The Horsehead nebula as a typical pillar in star forming regions

The Horsehead nebula appears on optical images as a dark patch of $\sim 5'$ extent against the bright HII region IC 434. Mid-infrared to submillimeter wavelength emissions from the gas and dust associated with this globule clearly indicate its morphology (see figure 1). A curved rim including the nose, ridge and mane of the horse is located at the western end of the nebula (*i.e.* the top of the head). This ridge is connected to the eastern L1630 molecular cloud by a thin filament, the horse throat. While optically thick tracers like the ^{12}CO lines show a low density halo surrounding the throat traced by the C^{18}O $J=2-1$ emission, optically thin tracers like the dust

¹ IRAM, 300 rue de la Piscine, 38406 Grenoble cedex, France

² LERMA-LRA, UMR 8112, CNRS, Observatoire de Paris and ENS, 24 rue Lhomond, 75231 Paris cedex 05, France

³ ESAC, Urb. Villafranca del Castillo, P.O. Box 50727, Madrid 28080, Spain

⁴ LUTH, UMR 8102, CNRS and Observatoire de Paris, Place J. Jansen, 92195 Meudon cedex, France

⁵ IAS, Université Paris-Sud, Bât. 121, 91405 Orsay, France

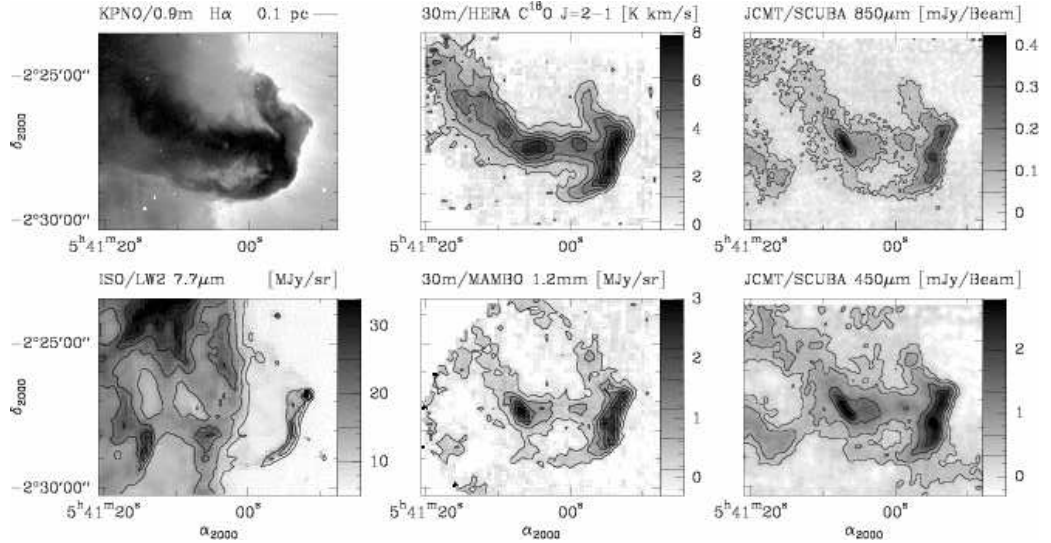


Fig. 1. $500'' \times 400''$ maps of the Horsehead nebula in different tracers: H α (resolution: $\sim 1''$, courtesy of Reipurth & Bally), $7.7\mu\text{m}$ aromatic continuum (resolution: $6''$, Abergel et al. 2003), $9.1\text{--}11.8\text{ km s}^{-1}$ C ^{18}O J=2–1 emission and 1.2 mm dust continuum (resolution: $11.7''$, Hily-Blant et al. 2005), $850\mu\text{m}$ and $450\mu\text{m}$ dust continuum (resolution: $15''$, courtesy of G. Sandell, published in Ward-Thompson et al. 2006). Values of contour level are shown on each image lookup table.

emission (from 1.2 mm to $350\mu\text{m}$) reveal the presence of two dense condensations: the first one associated with the western ridge, called B33-SMM1, and the second one in the middle of the throat, called B33-SMM2 (the ^{12}CO and $350\mu\text{m}$ images may be found in Pound et al. 2003 and in Philipp et al. 2006).

Two massive stars are located at the same projected distance of the Horsehead (0.5° or 3.5 pc at a distance of 400 pc), namely the O9.6Ib star ζOri north of the nebula and the O9.5V star σOri west of the nebula. However, figure 1 of Pound et al. (2003) shows that some molecular gas is located in projection between ζOri and the Horsehead nebula. Moreover, Hipparcos estimates of their distance (Perryman et al. 1997) indicate that ζOri ($250 \pm 50\text{ pc}$) is located further away from the Horsehead nebula than σOri ($352 \pm 113\text{ pc}$). Finally, Philipp et al. (2006) present in their figure 6 the image of the ^{12}CO J=4–3/J=2–1 ratio, which is an excellent tracer of the direction of the incoming far UV photons: Indeed, this ratio increases at the PDR edges due to the difference of optical depth between the two ^{12}CO transitions in regions with a steep temperature gradient. The ^{12}CO J=4–3/J=2–1 image clearly shows that the far UV illumination primarily comes from σOri , even though ζOri probably plays a role in the north rim of the nebula (*i.e.* the top of the neck).

Pound et al. (2003) were the first to cast the Horsehead nebula in the category of the pillars like the well-known examples in the Eagle nebula. They guess that the Horsehead nebula formed through the photoevaporation of low density material around the neck which was protected by the shadow of denser material in the ridge. The typical size and velocity gradients thus imply a formation timescale of $\sim 0.5\text{ Myr}$ and a timescale of destruction through photoablation of $\sim 5\text{ Myr}$. Hily-Blant et al. (2005) showed through careful measurement of velocity gradients in the C ^{18}O J=2–1 emission that the gas is rotating around the neck axis. The velocity gradients perpendicular to the neck axis are reasonably constant around an average value of $1.5\text{ km s}^{-1}\text{ pc}^{-1}$ (implying a rotation period of 4 Myr) except at the position of the dense condensation B33-SMM2, where the transverse velocity gradients experience a sharp increase up to $4\text{ km s}^{-1}\text{ pc}^{-1}$. The overall shape of the throat is thus assumed to be cylindrical with a fairly constant projected diameter of about $0.15\text{--}0.30\text{ pc}$. Since this study, Gahm et al. 2006 have confirmed that rotation of gas around pillar major axes is a common phenomenon. Hily-Blant et al. (2005) argued that the famous shape of the Horsehead nebula could derive from a pre-existent velocity field that progressively separated the mane and nose from the neck via the centrifugal effect.

In their simultaneous study of the CO and CI emissions, Philipp et al. (2006) deduce a total molecular mass of 24 M_\odot in the throat and 13 M_\odot in the outer halo. This leads to an upper limit (as the regions traced by C ^{18}O and CI may partially overlap) of the total mass of $\sim 37\text{ M}_\odot$. Ward-Thompson et al. (2006) derived the main characteristics of the two condensations of the Horsehead nebula. The eastern condensation (B33-SMM2)

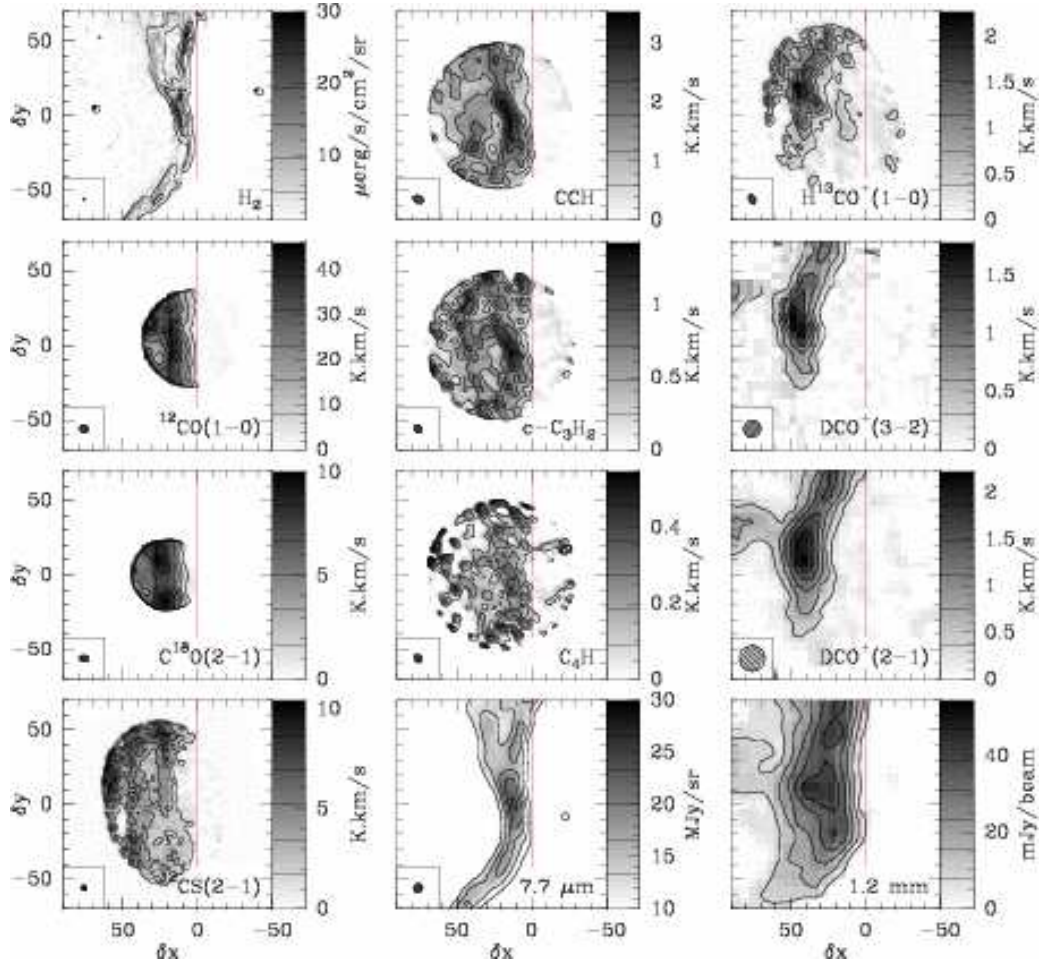


Fig. 2. Emission maps obtained with the IRAM Plateau de Bure Interferometer or 30m single-dish, except for the H_2 $v=1-0$ S(1) emission observed with the NTT/SOFI and the mid-IR emission observed with ISO-LW2. The image center is RA(2000) = 05h40m54.27s, Dec(2000) = -02°28'00''. The maps have been rotated by 14° counter-clockwise around the image center to bring the exciting star direction in the horizontal direction as this eases the comparison of the PDR tracer stratifications. Maps have also been horizontally shifted by 20'' to set the horizontal zero at the PDR edge delineated as the vertical red line. Either the synthesized beam or the single dish beam is plotted in the bottom left corner. The emission of all the lines is integrated between 10.1 and 11.1 km s^{-1} . Values of contour level are shown on each image lookup table (contours of the H_2 image have been computed on an image smoothed to 5'' resolution).

is seen in emission in the (sub)millimeter range and in absorption in the mid-infrared domain. Assuming a temperature of 15 K, its mass is $\sim 4 M_\odot$ in a region of dimension 0.15×0.07 pc. This yields an average H_2 density of 10^5 cm^{-3} while the peak density is $2 \times 10^6 \text{ cm}^{-3}$. Virial estimates imply that this dense core is in approximate gravitational equilibrium. The size of the western condensation (B33-SMM1) is 0.13×0.31 pc and its mass is $\sim 2 M_\odot$ (assuming a temperature of 30 K). This yields an average H_2 density of 10^4 cm^{-3} while the peak density is $6 \times 10^5 \text{ cm}^{-3}$. Its virial balance is however largely dominated by the ionizing radiation. Both condensations are potential progenitors of the next generation of star formation and may thus give clues about the differences between triggered and spontaneous star formation.

3 The Horsehead PDR as a chemical laboratory

The illuminated edge (PDR) of the western condensation presents one of the sharpest infrared filament (width: 10'' or 0.02 pc) detected in our Galaxy by ISOCAM. The most straightforward explanation given by Abergel et al. (2003) is that most of the dense material is within a flat structure viewed edge-on and illuminated in the plane of the sky by σ Ori. The H_2 fluorescent emission observed by Habart et al. (2005) is even sharper (width:

5''), implying the inclination of the PDR on the plane-of-sky to be less than 5° . The Horsehead ridge thus offers the opportunity to study at small linear scales (1'' corresponds to 0.002 pc at 400 pc) the physics and chemistry of a PDR with a simple geometry, very close to the prototypical kind of source needed to serve as a reference to chemical models. Since 2001, we started to study the Horsehead PDR mainly with the IRAM Plateau de Bure interferometer at 3 mm and the IRAM-30m at 1 mm achieving spatial resolutions from 3 to 11'' (except the H₂ fluorescent emission observed at 1''-resolution with the NTT/SOFI instrument). Figure 2 displays all the observed, high resolution maps already acquired. Those maps trace the different layered structures predicted by photochemical models according to chemistry networks, excitation conditions and radiative transfer.

Abergel et al. (2003) deduced from the distance between σ Ori and the PDR that the intensity of the incident far UV radiation field is $\chi \sim 60$ relative to the interstellar radiation field in Draine's units. Through the modelling of the H₂ and CO emission, Harbart et al. (2005) showed that the PDR has a very steep density gradient, rising to $n_{\text{H}} \sim 10^5 \text{ cm}^{-3}$ in less than 10'' (*i.e.* 0.02 pc), at a roughly constant pressure of $P \sim 4 \times 10^6 \text{ K cm}^{-3}$. These observations were followed by a chemical study of small hydrocarbons (CCH, c-C₃H₂, C₄H). Pety et al. (2005) showed that the abundances of the hydrocarbons are higher than the predictions based on pure gas phase chemical models (Le Petit et al. 2002 and reference therein). These results suggest that, in addition to gas-phase chemistry, another formation path of carbon chains should be considered in PDRs. Due to the intense far UV illumination, large aromatic molecules and small carbon grains may fragment and feed the interstellar medium with small carbon clusters and molecules in significant amounts. Recently, Goicoechea et al. (2006) showed that the gas sulfur depletion invoked to account for CS and HCS⁺ abundances is orders of magnitude lower than in previous studies of the sulfur chemistry (see also Goicoechea et al. in these proceedings). In this study, we have made a major step forward as we now have a non-LTE, non-local (Monte-Carlo) radiative transfer code which allows us to accurately bridge the gap between the modelled chemical abundances and the observed spectra. Finally, we observed the H¹³CO⁺ J=1-0 and DCO⁺ J=2-1 and J=3-2 lines during the winter and spring 2006. Our aim is to measure the fractional ionization across the western edge of the Horsehead nebula. The observed DCO⁺ lines are surprisingly strong (peak at 3 K) inside the dark part of the PDR, just $\sim 40''$ away from its illuminated edge. This opens the interesting possibility to probe at high resolution the chemical transition from far-UV photodominated gas to "dark cloud" shielded gas in a small field of view. All those results were unexpected, illustrating the importance of astrophysical references to constrain chemical models.

4 Conclusion

The PDR on top of the Horsehead nebula has a geometry not only well understood but also quite simple (almost 1D and viewed edge-on). The density profile across the PDR is well constrained and there are several current efforts to constrain the thermal profile. The chemistry of this source is even richer than expected as it brought numerous surprises. Finally, its combination of low distance to Earth (400 pc), low illumination ($\chi \sim 60$) and high density ($n \sim 10^5 \text{ cm}^{-3}$) implies that all the interesting physical and chemical processes can be probed in a field-of-view of less than 50'' with typical spatial scales ranging between 1 and 10''. All those properties make the Horsehead PDR a source ideally suited 1) for observation with current (*e.g.* PdBI) and future (*e.g.* ALMA) radioastronomy interferometers and 2) to serve as reference to models.

References

Abergel, A., Teyssier, D., et al. A&A, 410, 577
 Gahm, G. F., Carlqvist, P., Johansson, L. E. B., & Nikolić, S. 2006, A&A, 454, 201
 Goicoechea, J. R., Pety, J., Gerin, M., Teyssier, D., Roueff, E., Hily-Blant, P., & Baek, S. 2006, A&A, 456, 565
 Habart, E., Abergel, A., Walmsley, C. M., Teyssier, D., & Pety, J. 2005, A&A, 437, 177
 Hily-Blant, P., Teyssier, D., Philipp, S., & Güsten, R. 2005, A&A, 440, 909
 Le Petit, F., Roueff, E., & Le Bourlot, J. 2002, A&A, 390, 369
 Perryman, M. A. C., Lindegren, L., Kovalevsky, J., et al., 1997, A&A, 323, 49
 Pety, J., Teyssier, D., Fossé, D., Gerin, M., Roueff, E., Abergel, A., Habart, E., & Cernicharo, J. 2005, A&A, 435, 885
 Philipp, S. D., Lis, D. C., Güsten, R., Kasemann, C., Klein, T., & Phillips, T. G. 2006, A&A, 454, 213
 Pound, M. W., Reipurth, B., & Bally, J. 2003, AJ, 125, 2108
 Wakelam, V., Herbst, E., & Selsis, F. 2006, A&A, 451, 551
 Wakelam, V., Selsis, F., Herbst, E., & Caselli, P. 2005, A&A, 444, 883
 Ward-Thompson, D., Nutter, D., Bontemps, S., Whitworth, A., & Attwood, R. 2006, MNRAS, 369, 1201